

Seismic imaging of forearc backthrusts at northern Sumatra subduction zone

Ajay Chauhan, Satish C. C. Singh, Nugroho Hananto, Hélène Carton, Frauke Klingelhoefer, J.-X. Dessa, Haryadi Permana, N. J. White, David Graindorge

▶ **To cite this version:**

Ajay Chauhan, Satish C. C. Singh, Nugroho Hananto, Hélène Carton, Frauke Klingelhoefer, et al.. Seismic imaging of forearc backthrusts at northern Sumatra subduction zone. Geophysical Journal International, 2009, 179 (3), pp.1772-1780. 10.1111/j.1365-246X.2009.04378.x . insu-00445899

HAL Id: insu-00445899
https://insu.hal.science/insu-00445899

Submitted on 6 Aug 2020

HAL is a multi-disciplinary open access archive for the deposit and dissemination of scientific research documents, whether they are published or not. The documents may come from teaching and research institutions in France or abroad, or from public or private research centers.

L'archive ouverte pluridisciplinaire **HAL**, est destinée au dépôt et à la diffusion de documents scientifiques de niveau recherche, publiés ou non, émanant des établissements d'enseignement et de recherche français ou étrangers, des laboratoires publics ou privés.

Geophysical Journal International

Geophys. J. Int. (2009) **179,** 1772–1780 doi: 10.1111/j.1365-246X.2009.04378.x

Seismic imaging of forearc backthrusts at northern Sumatra subduction zone

Ajay P. S. Chauhan,[1] Satish C. Singh,[1] Nugroho D. Hananto,[1] Helene Carton,[2] F. Klingelhoefer,[3] J.-X. Dessa,[4] H. Permana,[5] N. J. White,[6] D. Graindorge[7] and SumatraOBS Scientific Team

[1]*Laboratoire de Géosciences Marines, Institut de Physique du Globe de Paris,* 4 *place Jussieu,* 75252 *Paris Cedex* 05*, France. E-mail: chauhan@ipgp.jussieu.fr*
[2]*Lamont-Doherty Earth Observatory,* 61 *Route* 9W - PO Box 1000, *Palisades,* NY 10964-8000, *USA*
[3]*Ifremer,* BP 70, 29280 *Plouzané, France*
[4]*Geosciences Azur,* BP 48, 06235 *Villefranche sur Mer, France*
[5]*LIPI, Jl. Sangkuriang, Bandung,* 40132, *Indonesia*
[6]*Bullard Laboratories, Department of Earth Sciences, University of Cambridge, Madingley Road, Cambridge* CB3 0EZ, *UK*
[7]*Université de Bretagne Occidentale, Place Nicolas Copernic,* 29280 *Plouzané, France*

Accepted 2009 September 2. Received 2009 August 21; in original form 2009 April 12

SUMMARY

Forearc tectonics at accretionary convergent margins has variously been studied using analogue and numerical modelling techniques. Numerous geophysical investigations have targeted the subsurface structure of active forearc settings at convergent margins. However, several critical details of the structure, mode of tectonic evolution and the role forearcs play in the subduction seismic cycle remain to be further understood, especially for large accretionary margins. In this study, we present a high-resolution deep seismic reflection image of the northern Sumatran subduction forearc, near the 2004 December 26 Sumatra earthquake epicentral region. The profile clearly demarcates the backthrust branches at the seaward edge of the Aceh forearc basin, along which the inner forearc continues to evolve. Sharp bathymetric features at the seafloor suggest that the imaged backthrusts are active. Coincident wide-angle seismic tomographic image of the Sumatra forearc allows us to image the geometry of the seaward dipping backstop buttress, with which the imaged backthrust branches are associated. The presence of forearc backthrusting confirms model predictions for the development of backthrusting over seaward dipping backstops. The West Andaman fault at the seaward edge of Aceh basin appears to be a shallow tributary of the backthrust and sheds light on the complex deformation of the forearc. Uplifting along the backthrust branches may explain the presence of forearc islands observed all along Sumatran margin and help further constrain the tectonic models for their evolution. Moreover, if these backthrusts slip coseismically, they would contribute to tsunamigenesis and seismic risk in the region.

Key words: Forearc backthrusting; Seismic reflection image; Seismic tomography; Subduction zone processes.

1 INTRODUCTION

In subduction thrust settings, about ~8200 km of the length of convergent margins are marked by the presence of large accretionary wedges (von Huene & Scholl 1991). The growth of accretionary wedges is governed by the process of removal of sediments from the downgoing slab and their attachment to the upper plate referred to as subduction accretion (Scholl *et al.* 1980), which can occur as sediment underplating beneath the wedge or by frontal accretion (Platt 1989). Alternatively, sediment mass along with the downgoing oceanic slab is subducted beneath the overlying plate by the process of sediment subduction (Shreve & Cloos 1986; von Huene & Scholl 1991). For a large accretionary wedge, there could be a significant surface erosion as well. At several convergent margins, subduction erosion processes dominate, which mark the removal of material from the upper plate (von Huene & Scholl 1991). The mass balance for large parts of those convergent margins, where wide accretionary wedges exist, is distinguished by net subduction accretion at geological timescales (Clift & Vannucchi 2004), posing unique conditions for subduction contact. Accretionary wedge mechanics is usually modelled in terms of critical wedge theory (Dahlen 1990; Wang & Hu 2006), which provides a conceptual framework for the relation between basal dip, wedge taper, stress regime and frictional strengths of wedge and basal mass. Understanding the dynamics

© 2009 The Authors
Journal compilation © 2009 RAS

Downloaded from https://academic.oup.com/gji/article-abstract/179/3/1772/782446 by CNRS - ISTO user on 06 August 2020

of accretionary wedges and the forearc has been a recurring theme owing to their importance for (1) quantifying the factors dictating forearc deformation patterns, (2) the role forearc structure plays in defining the seismogenic locked zone and the associated subduction seismic cycle (Byrne *et al.* 1988; Fuller *et al.* 2006; Wang & Hu 2006).

Inner forearc deformation patterns have been widely studied using analogue and numerical modelling techniques explaining several geological observations, and predicting possible mechanisms for forearc evolution (Byrne *et al.* 1993; Willett *et al.* 1993; Lallemand *et al.* 1994; Wang & Davis 1996; Beaumont *et al.* 1999). On its landwards edge the accretionary wedge usually culminates at the forearc high that evolves against the backstop buttress, defined as material with higher yield strength as compared to the wedge material trenchwards of it (Silver & Reed 1988; Byrne *et al.* 1993; Beaumont *et al.* 1999). The backstop buttress could be either of continental or sedimentary origin. Seismic studies have imaged the landward dipping backstop and associated accretionary complex in Cascadia (Tréhu *et al.* 1994), and seaward dipping backstop structure in Lesser Antilles subduction zone (Bangs *et al.* 2003; Westbrook *et al.* 2008), south Sumatra and Java (Kopp & Kukowski 2003). The presence of backthrusting within the accretionary wedge has been observed along segments of the Sunda Arc (Karig *et al.* 1980; Silver & Reed 1988), however its relationship with backstop is not clearly defined, particularly at depth.

Northern Sumatra subduction megathrust is one of the largest accretionary margins anywhere on the planet, with the lateral extent of wedge being from 160 to 180 km (Singh *et al.* 2008), comparable to the accretionary wedges observed in Java (Schluter *et al.* 2002; Kopp & Kukowski 2003) and at Aleutian margin (Clift & Vannucchi 2004). It is also a very active subduction setting generating one of the largest earthquakes ever recorded on 2004 December 26 with an estimated magnitude of M_w 9.3 (Ammon *et al.* 2005), comparable to the great earthquakes of Alaska in 1964 (M_w 9.2) and Chile earthquake of 1960 (M_w 9.5) (Ishii *et al.* 2005). The Sumatra–Andaman earthquake resulted in a massive tsunami that caused immense destruction along the coastlines of Southeast Asia (Geist *et al.* 2007). The region has been the subject of surface morphological studies (Henstock *et al.* 2006; Graindorge *et al.* 2008), and subsurface investigations of limited resolutions (Fisher *et al.* 2007; Seeber *et al.* 2007). Sumatra megathrust provides a unique opportunity to understand the forearc deformation processes along an obliquely convergent boundary where the downgoing plate transports about 5 km of sediment thickness forming a rapidly evolving accreting margin (Singh *et al.* 2008).

We present results from a portion of a combined deep seismic reflection and refraction survey at the northern Sumatra subduction system, elaborating on the backstop geometry and related backthrust branches. We correlate the imaged backthrusts with bathymetric features and published regional aftershock patterns to identify its activity. Measured geological uplift rates of forearc islands and their coseismic uplift patterns provide additional constraints on the backthrust activity, highlighting the role backthrusts play in the evolution of the forearc ridge and slip-partitioning. We discuss the role backthrusts may play if they rupture coseismically during megathrust events, with substantial consequences for tsunami generation.

2 STUDY AREA

The study area is located offshore the northern tip of Sumatra Island, where the Indo-Australian plate obliquely subducts underneath the overriding Sunda plate at a rate of ∼50–55 mm yr^{-1} (Prawirodirdjo & Bock 2004). This segment of the Sumatra subduction system broke during the 2004 December 26 earthquake, from Simeulue to Andaman Islands (∼1300 km) (Ammon *et al.* 2005). All the rupture models for the 2004 December 26 event predict an area of high slip ∼150 km north of the epicentre (Ammon *et al.* 2005; Chlieh *et al.* 2007). The corridor located offshore the northern tip of Sumatra is thus well suited to study the structure of the subduction megathrust and further investigate the tsunami source localization. Fig. 1 displays the bathymetric map of the study area, which highlights active deformation at subduction front, a very wide accretionary wedge, forearc ridge in line with Simeulue-Nicobar islands, West Andaman fault (WAF) traces, Aceh forearc basin, and the right-lateral Sumatra fault nearly coincident with the volcanic arc. Slip vectors of recorded seismicity and geodetic measurements indicate that slip-partitioning is almost complete at the megathrust (McCaffrey *et al.* 2000). The strike parallel component of convergence is taken up on-land by the Sumatra fault with variable rates of slip and associated seismicity (Sieh & Natawidjaja 2000).

In July–August 2006, a coincident deep seismic refraction and reflection profile was shot using the French R/V Marion Dufresne and the WesternGeco M/V Geco Searcher vessel carrying 8260 (∼135.35 litre) and 10170 (∼163.87 litre) cubic inch sources, respectively. The 520-km-long profile is oriented ∼20° anticlockwise from the trench normal on which 56 ocean-bottom seismometers (OBS) spaced at 8.1 km were deployed and shots were fired at 150 m intervals (Fig. 1). A 12-km-long streamer was used for the reflection survey at 50 m shot interval, to image the deeper structure of the megathrust (Singh *et al.* 2008). For deep seismic reflection study, the air gun array and long streamer (12 km) were towed at 15 m water depth, providing dominant frequency at 25 Hz for imaging deep structures (Singh *et al.* 2008). Another 5.5-km-long streamer was towed at 7.5 m water depth to acquire high-resolution data with a dominant frequency of 50 Hz, to better image the near surface features (sediments and faults).

3 SEISMIC REFLECTION RESULTS

To image deeper structures, where low-frequency energy dominantly penetrates, the seismic reflection data acquired on the 12 km streamer were resampled to 8 ms from 2 ms sampling length, consistent with a bandwidth of 5–40 Hz. The data were also decimated to a 25 m group interval, yielding a common midpoint (CMP) spacing of 12.5 m, sufficient for deep structural imaging. Seismic processing steps included swell noise attenuation, multiple suppression using iterative Radon filtering, velocity analysis at 1 km spacing and stacking of the 120-fold data. Post-stack 2-D Kirchhoff migration was applied using a smooth velocity model based on picked velocities (Singh *et al.* 2008). To obtain a complementary higher resolution image of the near surface features the 5.5 km data set was sampled at 4 ms, with a group interval of 12.5 m and corresponding CMP spacing of 6.25 m. This data set was also processed and post-stack time migrated using similar processing flow steps as described above.

The time-migrated seismic reflection image of the Sumatran forearc is shown in Figs 2 and 3. The Aceh forearc basin contains 1 s sediments. The upper sediments are nearly flat although lower sediments show some sign of folding. The acoustic basement is clearly imaged, which seems to be connected with a reflection that continues down to 8 s two-way traveltime (TWTT). There is a veneer of thin sediments (150 ms) on NE slope of the forearc ridge. The slope break is marked by a small basin (distance 183 km), which

Downloaded from https://academic.oup.com/gji/article-abstract/179/3/1772/782446 by CNRS - INSTO user on 06 August 2020

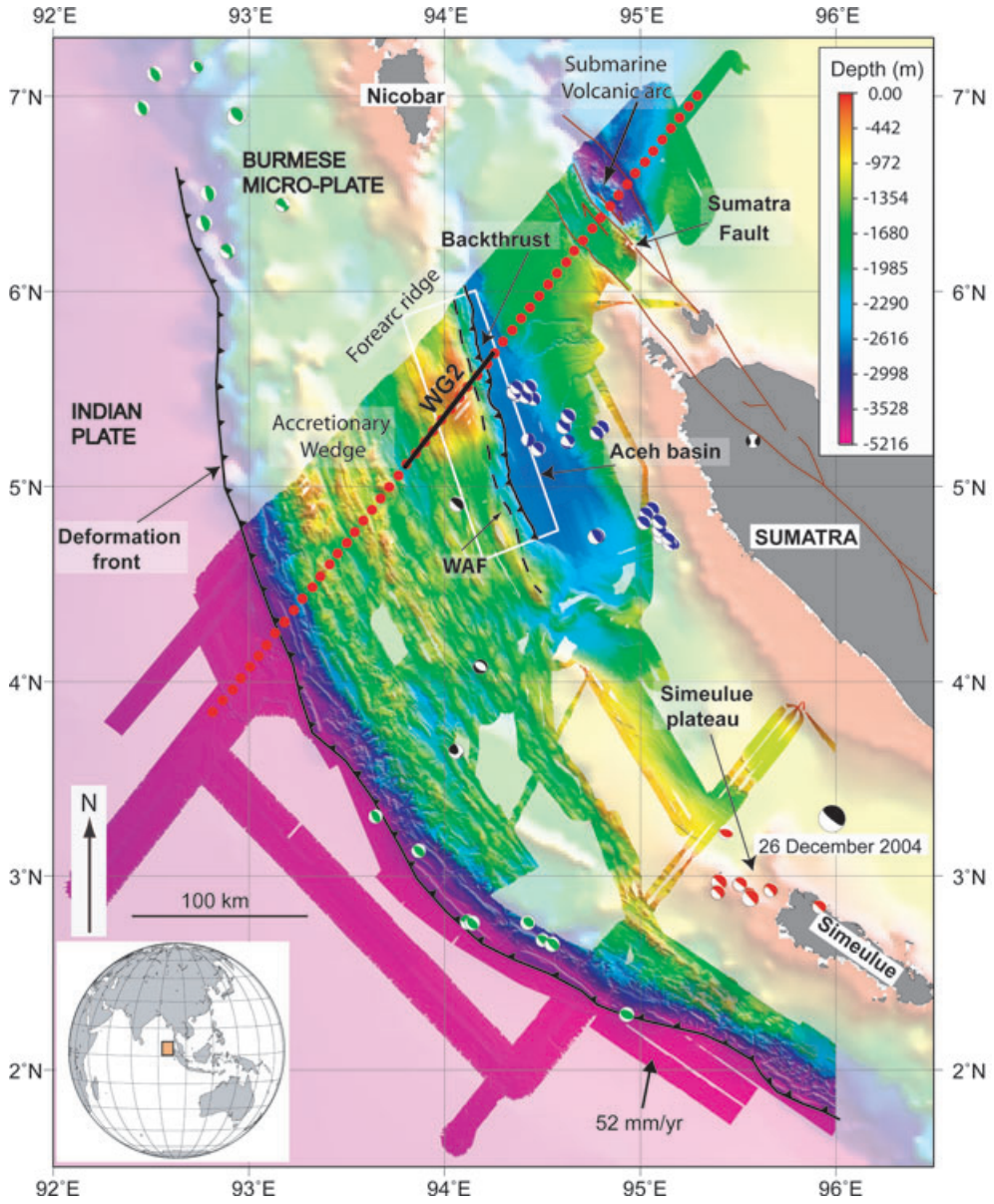


Figure 1. Map of the study area, bathymetry compiled from the data acquired by the British (Henstock *et al.* 2006) and the French surveys (Singh *et al.* 2005), with GEBCO data set in background. The OBS positions are marked by red circles, section of the WG2 seismic profile presented is marked as black line. Aftershock locations from EHB catalogue are plotted with corresponding Harvard CMT solutions. Blue events are underneath the Aceh forearc, red around Simeulue plateau, green events at the deformation front and black are other miscellaneous events. Location of the 2004 December 26 main event has also been marked. WAF: West Andaman Fault. Inset shows the location of study area on the Earth. White box shows the region in Fig. 3(a).

has been identified as a small pull-apart basin associated with the WAF (Seeber *et al.* 2007). Based on the bathymetry image (Fig. 3a), Singh *et al.* (2005) interpreted this feature as a lithospheric scale boundary. The high-resolution seismic image (Fig. 3c) suggests that it could be due to a combination of small pull apart and push-up ridge, leading to an inverse flower structure, which is generally associated with a strike slip fault. The shallowest part of the forearc ridge (∼ distance 152–175 km) is underlain by 1–1.5 s thick folded and faulted sediments, where the acoustic basement is also heavily deformed. The acoustic basement is near the seafloor along the rest of the forearc ridge (∼ distance 125–150 km). The presence of deformed sediments at the shallowest part of the forearc ridge surrounded by acoustic basement near the seafloor suggests that the forearc ridge has been uplifted. Both bathymetry and seismic reflection data suggest that NE margin of the forearc ridge is steeper than that on SW side of the ridge, implying that uplift is dominant on the NE side of the ridge.

Below the acoustic basement, the reflectivity is very poor. However, two strong seaward-dipping reflections are imaged beneath the shallowest portion of the forearc ridge towards and beneath NE margin of the ridge. These reflections are imaged down to 8 s. The upper reflection event reaches its shallowest point below the slope of the forearc ridge (Fig. 3a), where the WAF was identified in bathymetric and single-channel seismic data (Curray *et al.* 1979; Singh *et al.* 2005; Seeber *et al.* 2007). It seems to branch into thrust and normal faults near the seafloor, resulting in the flower structure (Fig. 3c). The lower reflection event continues up to the base of the Aceh basin sediment fill, and seems to branch onto an active

Downloaded from https://academic.oup.com/gji/article-abstract/179/3/1772/782446 by CNRS - ISTO user on 06 August 2020

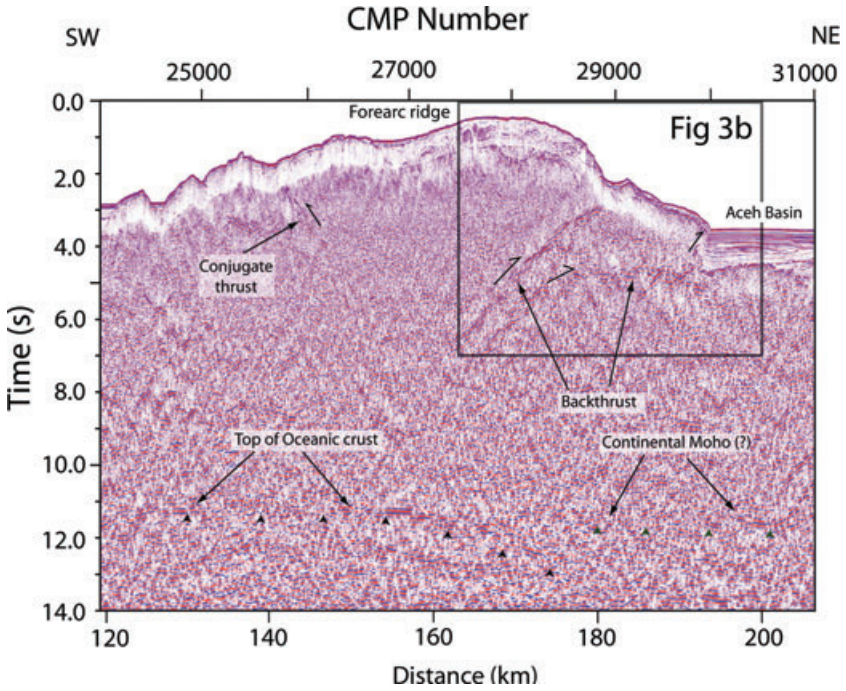


Figure 2. Time-migrated seismic image of part profile WG-2 at the Sumatran forearc, location on Fig. 1. The data were processed using a standard processing technique (Singh *et al.* 2008). Black and green triangle pointers have been marked to highlight reflections from the top of downgoing oceanic crust and the continental upper plate moho, respectively. All distances marked are from the subduction front. Vertical exaggeration is 1:6 at 1.5 km s^{-1}.

backthrust marking the edge of the basin, earlier observed on the bathymetric data (Singh *et al.* 2005) and previously acquired seismic profiles (Malod & Kemal 1996). Localized deformation at the western edge of the Aceh forearc basin can be observed along the lower reflection, marked in Fig. 3c along the green contours for sediment horizons. These results combined with the near surface information above suggest that these two reflections are seaward dipping backthrust responsible for uplifting of the forearc ridge. On the SW side of the forearc ridge, a landward dipping reflection event is imaged, which could be a conjugate thrust.

A band of strong reflection energy is observed at 11 s TWTT (distance 125–175 km, Fig. 2) beneath the forearc ridge, which is at appropriate depth for the downgoing oceanic crust (Singh *et al.* 2008; Dessa *et al.* 2009). Although the coherency of reflections is poor beneath NE slope of the forearc ridge, they seem to dip towards land beneath the shallowest portion of the forearc ridge as expected for the downgoing oceanic crust, similar to that observed further south near the epicentral region (Singh *et al.* 2008). Beneath the NE slope of the forearc ridge and Aceh basin, a sub-horizontal reflection is observed at 11 s TWTT, which could be the reflection from the continental Moho.

4 WIDE ANGLE SEISMIC TOMOGRAPHIC RESULTS

Performing the tomographic inversion of a 520-km-long profile that traverses the 5–7 km thick oceanic crust, 10–20 km thick accretionary prism sediments, continental crust and volcanic arc is a challenging task. The OBS recorded energy to offsets that varied from 40 km to 150 km, depending upon the subsurface structure. For example, the OBS placed on the forearc ridge (Fig. 4a) recorded arrivals from accreted sediment to an offset of 50 km towards SW, whereas the same OBS recorded crustal arrival (Pg) to an offset of 80 km (Fig. 4b) towards NE. First arrival traveltime picks were made manually on the 51 OBSs which had useful data, with about ∼30 000 picks in total, used as input for tomographic inversion. To obtain the tomographic image of the subsurface from the traveltime picks data an adaptive traveltime inversion algorithm was implemented (Trinks *et al.* 2005). The velocity cells were parametrized with an adaptive triangular gridding scheme, the starting value for the triangle side was chosen as 5 km. The adaptive triangle side width was successively refined to 2.5 km and 1.25 km with smoothing regularization oriented accordingly, to obtain the final velocity model (Figs 4 and 5a). The root mean square misfit of the final model was reduced to 132 ms, where picking uncertainties are in 80–200 ms range. In Fig. 4b, we show the fit between observed and calculated arrival times for the final model for OBS 27 placed on the forearc ridge (Fig. 4a). Fig. 4(a) shows the ray coverage within the study area for all the OBS to highlight the accuracy of the tomographic model. The ray diagram clearly shows that the resolution is very high down to 10 km and the OBS data provide the *P*-wave velocity model to depths of upto ∼30 km; here we elaborate on the structure of the forearc region only (Fig. 5a).

The 3 km s^{-1} velocity contour gently follows the seafloor topography, and is thickest beneath shallowest part of the forearc ridge where folded and faulted sediments were imaged (Fig. 3b), suggesting the presence of relatively un-compacted sediments. The 4 km s^{-1} velocity contour shows similar features. However, it seems to correspond to the basement imaged beneath the Aceh basin on seismic reflection profile (Fig. 3). By contrast, the 5 km s^{-1} velocity contour significantly departs from a seafloor-parallel pattern; it is ∼3 km below seafloor (bsf) beneath the Aceh basin, however suddenly deepens to ∼10 km bsf under the forearc ridge. The 6 km s^{-1} velocity contour shows a similar behaviour. A reverse pattern through the forearc basin/ridge transition is observed at the 7 km s^{-1} contour, which lies 10 km below the 6 km s^{-1} contour beneath the Aceh basin, however decreases to 5 km below the 6 km s^{-1} contour beneath the forearc ridge. It is always difficult to

Downloaded from https://academic.oup.com/gji/article-abstract/179/3/1772/782446 by CNRS - INSTO user on 06 August 2020

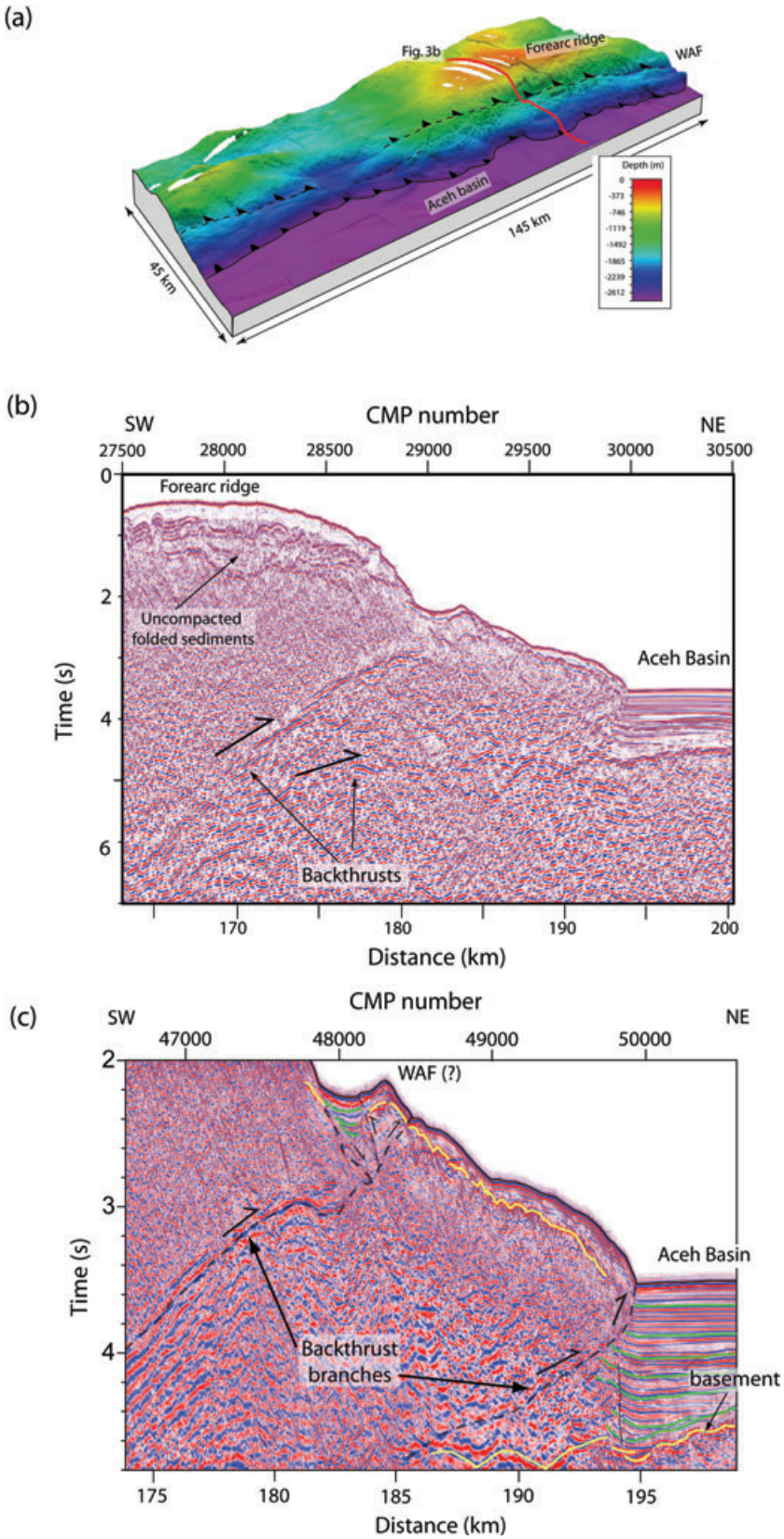


Figure 3. (a) 3-D perspective view of surface features related to backthrusting at the Sumatran forearc on bathymetry section, from SE Aceh basin. Location of seismic line shown in Fig. 3b is marked. (b) Blow-up seismic image in the time domain showing the backthrust faults (arrows), horizontal sediments in Aceh basin and folded sediments on the fore arc high (boxed area on Fig. 2). (c) Interpreted image of the high-resolution time-migrated seismic section of near surface features at the forearc obtained by 5.5 km streamer data set. Backthrust branches have been marked, location of WAF indicated as interpreted in earlier studies (Curray *et al.* 1979; Singh *et al.* 2005; Seeber *et al.* 2007). Green contours mark sediment horizons in Aceh basin. Yellow contour marks the basement reflections.

© 2009 The Authors, *GJI*, **179,** 1772–1780
Journal compilation © 2009 RAS

Downloaded from https://academic.oup.com/gji/article-abstract/179/3/1772/782446 by CNRS - ISTO user on 06 August 2020

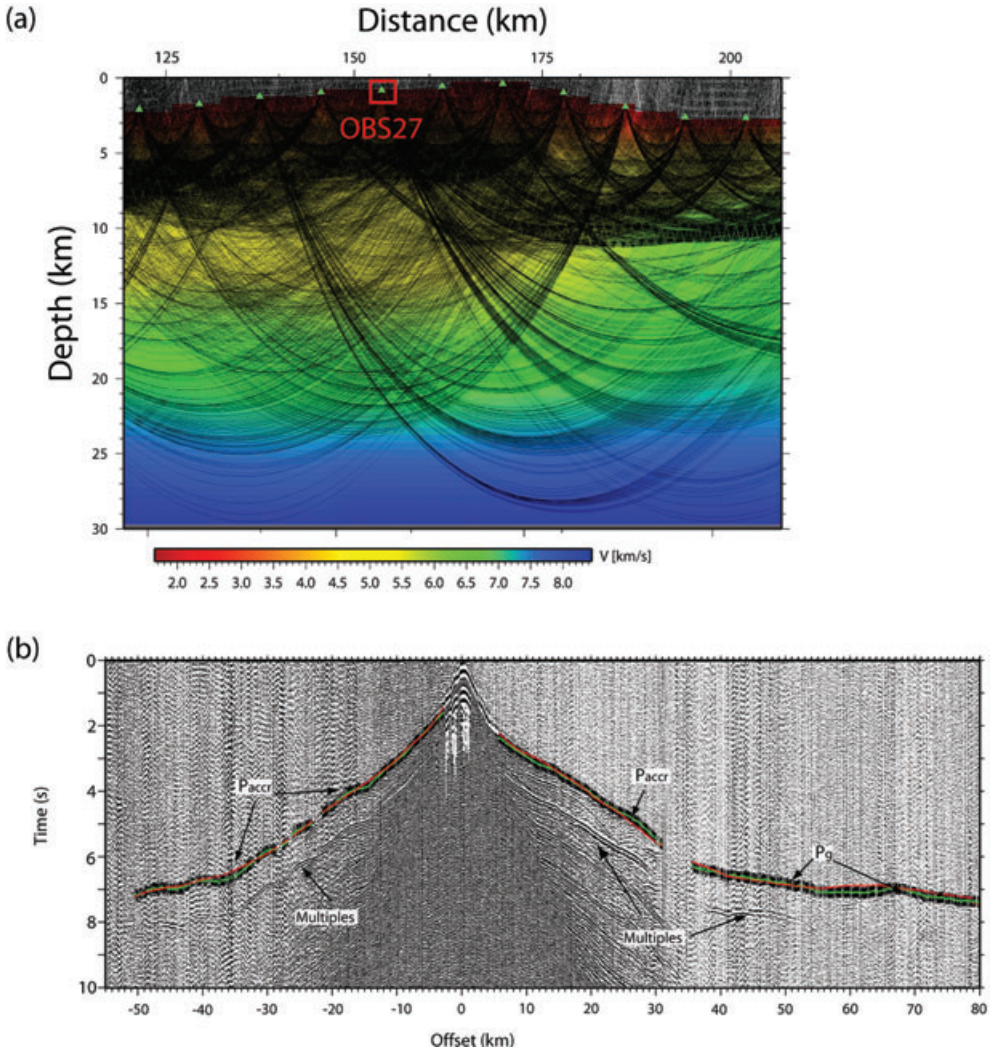


Figure 4. (a) Ray coverage within the velocity model presented in this study (Fig. 5a), position of OBS 27 has been marked. (b) OBS 27 seismic record plotted at reduced velocity of 8 km s^{-1}, various picked phases and multiples have been marked. The picked arrival times (green) and predicted from the inverted velocity model (red) are plotted, picking uncertainty shown as the error bar. P_{accr}: refractions from accreted sediments, P_g: refractions from crust.

demarcate precise structural boundaries on the smooth velocity models provided by tomographic methods. Nonetheless, the tomographic image obtained here suggests that the Aceh basin is underlain by a high-velocity basement of continent crustal origin and possibly a continental backstop buttress beneath the north-eastern slope of the forearc ridge. The flat character of the 8 km s^{-1} contour may be due to the proximity of continental and oceanic mantle, sparse ray coverage at that depth and lateral smoothing applied in the inversion (Trinks *et al.* 2005).

The time-migrated deep seismic reflection image was depth converted (Fig. 5b) using the velocity model derived from tomographic inversion (Fig. 5a). Because the seafloor topography is complex and the tomographic velocity model is smooth, reflections from deeper events have been slightly distorted through post-stack depth conversion (Fig. 5b). We discuss the joint interpretation of the two results in the next section.

5 COMBINED INTERPRETATION

The combined interpretation of seismic reflection and tomographic images allows us to define the structural boundaries much more precisely (Figs 5a and b). We interpret the reflections from the basement beneath the Aceh Basin and lower backthrust as the continental backstop (Fig. 5c). The velocity just below these reflections is slightly lower (4 km s^{-1}) than expected for continental crust, however this could be due to the vertical smoothing. The continental crust underneath the Aceh basin is marked by a high vertical velocity gradient within the first 10 km, similar to high-velocity gradient observed in upper crystalline crust in other instances (McCaughey *et al.* 2000). Beneath the Aceh basin and forearc ridge, there is a band of reflectivity at ∼25 km depth (11 s), which we interpret as the continental Moho. The velocity at this interface is slightly lower (∼7.5 km s^{-1}), which could again be due to a smoothing effect. There is a weak reflection at ∼20 km depth (9 s) near the 7 km s^{-1} velocity contour, which could be another candidate for the continental Moho, or some intracrustal feature. In any case, the continental crust is thin beneath the Aceh basin (18–23 km), which is consistent with the crustal thickness observed farther south on deep seismic reflection and tomographic results (Singh *et al.* 2008; Dessa *et al.* 2009). The downgoing oceanic crust is marked by a combination of reflectivity and high velocity (7.0–7.5 km s^{-1}); it overlies the oceanic mantle marked by a velocity of 8 km s^{-1}, and intersects the continental Moho at ∼25–27 km depth (11 s).

© 2009 The Authors, *GJI*, **179,** 1772–1780
Journal compilation © 2009 RAS

Downloaded from https://academic.oup.com/gji/article-abstract/179/3/1772/782446 by CNRS - INSTO user on 06 August 2020

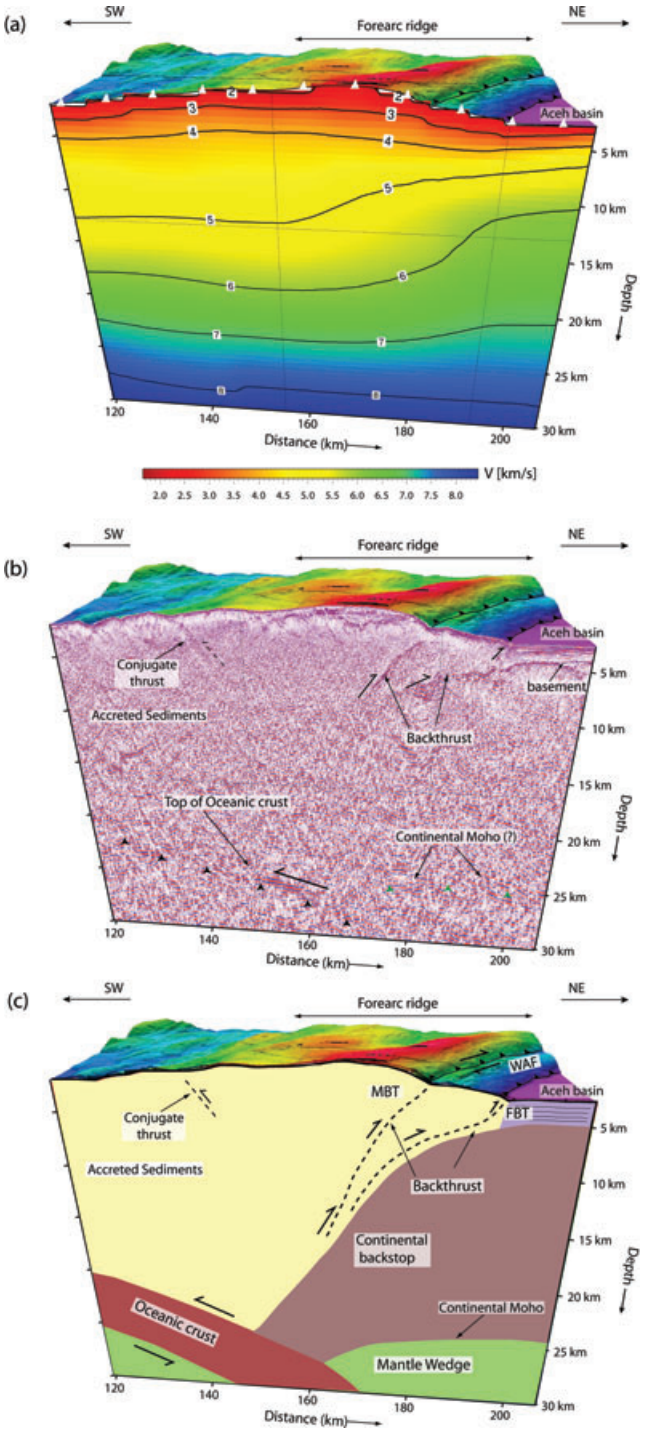


Figure 5. (a) 3-D block diagram showing the *P*-wave velocity model obtained by first arrival traveltime tomography along the black line on Fig. 1, and seafloor bathymetry. All distances marked are from the subduction front. Contours are marked for every 1 km s^{-1}. The water depth varies from ∼2700 m in the Aceh basin (purple) to ∼255 m on forearc ridge (red). White triangles are the positions of OBSs within the length (87.5 km) of the profile shown. (b) 3-D block diagram of depth converted seismic reflection image of Fig. 2b. Locations of backthrusts, conjugate fault, reflections from top of the oceanic crust and continental Moho have been marked. Black and green triangle pointers have been marked to highlight reflections from the top of downgoing oceanic crust and the continental moho, respectively. (c) Schematic diagram of interpreted tectonic features at the forearc high of the north Sumatra Margin. Continental backstop and Moho are determined from the interpretation of the seismic reflection and refraction results.

We suggest that the upper backthrust reflection event is the main backthrust (MBT) bounding the internal deformation zone along which the inner forearc wedge continues to deform. Thick high-velocity accreted sediments (3–5 km s^{-1}) lie to the immediate southwest of the MBT, suggesting that these sediments have been highly compacted. The southwestern side of the forearc ridge seems to be bounded by a landward dipping thrust, which might be a conjugate fault. We call the lower backthrust, which emerges at the seafloor on the southwest border of the Aceh basin, the frontal backthrust (FBT). On its eastern edge, the FBT deforms the sediment horizons of the Aceh forearc basin (Fig. 3c) in its near surface reaches, showing localized deformation patterns seawards of the forearc basin that confirm predictions from numerical studies on bivergent wedges (Willett *et al.* 1993). Our results, which clearly demarcate the presence of backthrusts associated with a seaward dipping backstop, also confirm results from analogue modelling studies which predict that seaward dipping backstops are indeed conducive for the development of backthrust structures along which the inner forearc deforms (Byrne *et al.* 1988; Wang & Davis 1996).

Our results suggest that the backthrusting extends down to 15 km. The dip of the backthrust is about ∼25–30°, with less steep angles in the shallower zone. In the vicinity of the epicentral region of the 2004 December 26 earthquake, Singh *et al.* (2008) have imaged a now inactive backthrust located in the Simeulue forearc basin at ∼170 km from the trench. Further south, based on field geological work, presence of backthrusting has been inferred on the northeastern edge of the Nias Island (Karig *et al.* 1980; Silver & Reed 1988; Briggs *et al.* 2008). Taken together, these results suggest that seaward dipping backthrusts are persistent feature along the northern Sumatra subduction zone at the northeast side of forearc ridges and islands.

6 BACKTHRUSTING AND FOREARC EVOLUTION

Teleseismic aftershocks do not show any shallow events that could be associated with the forearc backthrust, however display a deeper band of thrust activity underneath the forearc in the vicinity of the plate contact (Engdahl *et al.* 2007) (Fig. 1). However, regional aftershock studies using OBS data indicate the presence of seismic events underneath the forearc ridge (Araki *et al.* 2006; Sibuet *et al.* 2007) with a group of shallow events near our proposed backthrust structure, suggesting that these faults are seismically active. Using 3-D velocities for their revised relocation of aftershocks recorded after the 2004 December 26 event, Lin *et al.* (2009) have reported the presence of an active backthrust at the western edge of the Aceh basin. Sharp bathymetric lineaments, at the seaward edge of the Aceh basin, can be traced for upto ∼150 km where the FBT arrives at the sea floor, which indicate that FBT is active (Figs 1 and 2). The MBT branch arrives at the sea floor where WAF was previously identified using bathymetric, morphological and shallow seismic reflection profiles (Singh *et al.* 2005; Seeber *et al.* 2007).

Further south, forearc islands present along the northern Sumatra margin have been documented to be uplifting during the recent geological past, and are reported to have uplifted coseismically during recent Sumatra events (Vita-Finzi 2007; Briggs *et al.* 2008). Briggs *et al.* (2008) estimate the average Holocene uplift rates for Nias to be about ∼0.5 mm yr^{-1} (maximum rates ∼1.5 mm yr^{-1}), which they attribute to elastic uplifting. However, alternative models of deformation patterns on Nias (Karig *et al.* 1980; Vita-Finzi 2007), and the recorded coseismic uplifts of Nias and Simeulue islands

Downloaded from https://academic.oup.com/gji/article-abstract/179/3/1772/782446 by CNRS - ISTO user on 06 August 2020

favour the possibility of active backthrusting. The slip along the active backthrust could either be aseismic or co-seismic. The uplifted folded and faulted sediments on the forearc ridge (Fig. 3b) and the link between the backthrust image and sharp bathymetric features at SW side of the Aceh basin (Fig. 5b) suggest that the forearc ridge is uplifting in a manner similar to the Simeulue and Nias islands along the backthrust.

The WAF, which has been proposed to be as a lithospheric-scale boundary, appears to be a tributary of the backthrust structure (Singh *et al.* 2005); and dextral slip along WAF, if any, is yet to be estimated. Our data do not allow us to image a vertical fault that might be associated with a strike slip fault. Therefore, we suggest that the backthrust is the dominant tectonic structure controlling the surface expression of displacement and resulting ridge-like features along the WAF, observed as flower structure on seismic reflection images (Malod & Kemal 1996; Singh *et al.* 2008). The exact spatial and temporal relationship of the backthrust and WAF is difficult to estimate based on just bathymetric and seismic data sets. The relationship is intricate and deserves further investigation to obtain comprehensive understanding of slip partitioning.

7 DISCUSSION AND CONCLUSIONS

Our results suggest that at north Sumatra megathrust, uplifting of inner forearc ridge occurs along active backthrust branches, which are associated with continental backstop lying underneath Aceh forearc basin. We confirm model predictions that seaward dipping backstops are conducive to backthrusting along which the forearc continues to deform (Silver & Reed 1988; Byrne *et al.* 1993). The uplifting of the inner forearc has been observed in both interseismic and coseismic periods resulting in the formation of forearc islands. Seismicity and sharp bathymetric features indicate that the backthrusting is persistent feature along the Sumatra megathrust, and is capable of accommodating such slip.

These results are in conformation with similar observations made earlier based on field investigations along the sunda arc (Karig *et al.* 1980; Silver & Reed 1988). Similar to backthrusting within bivergent wedges on-land (Silver & Reed 1988), backthrusting within the accretionary wedges at subduction margins has been observed in other instances, for example Lesser Antilles accretionary wedge (Torrini & Speed 1989). The deep sub-surface seismic image of backthrusts, related with the seaward dipping backstop presented here, strengthens the argument that backthrusting is an important tectonic process at accretionary convergent margins. Forearc structures are known to have first-order influence on defining the limits of the seismogenic locked zone of subduction thrust faults (Byrne *et al.* 1988; Fuller *et al.* 2006; Wang & Hu 2006). Our results add to the knowledge of forearc tectonics at the northern Sumatra margin, and will provide further constraints to address questions regarding seismogenic behaviour of Sumatra subduction system.

These results have important implications for forearc processes and tsunamigenesis. In case of the 2004 December 26 tsunami, based on early tsunami arrival times and high run-up heights in the near field, Plafker *et al.* (2006) postulated the presence of a secondary tsunami source near the forearc ridge. Sea surface heights measured on transect of Jason-1 satellite recorded double-peaked lead wave suggesting the possibility of a dual source for this tsunami (Smith *et al.* 2005). Coseismic slip along the imaged backthrust during the 2004 earthquake might provide a geologically viable secondary source and improve the understanding of the tsunami. Simultaneous slip on backthrust faults might be difficult to notice on seismological records of the main earthquake, as these faults dip in a nearly orthogonal direction to the megathrust. Simultaneous conjugate earthquake slip has been observed in other instances (Robinson *et al.* 2001). If slip along backthrusts indeed occurs coseismically, then it might have wider implication for subduction zones of similar constitution, and should be paid attention to while designing the networks of early tsunami warning system.

ACKNOWLEDGMENTS

We thank the Captain and crew of the R/V Marion Dufresne for their professional support to conduct the SumatraOBS experiment. The ocean bottom seismometers utilized in this study were provided by INSU, Ifremer and the UK-OBIC facilities. We sincerely thank Schlumberger for their generosity to help with seismic reflection data acquisition and processing. Relocated earthquake locations from the EHB catalogue were kindly provided by Bob Engdahl. The manuscript was improved by comments from editors J. Virieux, T. Becker and three anonymous reviewers. This is IPG Paris contribution 2544.

REFERENCES

Ammon, C.J. *et al.*, 2005. Rupture process of the 2004 Sumatra-Andaman earthquake, *Science,* **279,** 143–167.

Araki, E., Shinohara, M., Obana, K., Yamada, T., Kaneda, Y., Kanazawa, T. & Suyehiro, K., 2006. Aftershock distribution of the 26 December 2004 Sumatra-Andaman earthquake from ocean bottom seismographic observation, *Earth Planets Space,* **58,** 113–119.

Bangs, N.L., Christeson, G.L. & Shipley, T.H., 2003. Structure of the Lesser Antilles subduction zone backstop and its role in a large accretionary system, *J. geophys. Res.,* **58,** 113–119.

Beaumont, C., Ellis, S. & Pfiffner, A., 1999. Dynamics of sediment subduction-accretion at convergent margins: short-term modes, long-term deformation, and tectonic implications, *J. geophys. Res.,* **104,** 17 573–17 601.

Briggs, R.W. *et al.*, 2008. Persistent elastic behavior above a megathrust rupture patch: Nias island, West Sumatra, *J. geophys. Res.,* **113,** B12406.

Byrne, D.E., Davis, D.M. & Sykes, L.R., 1988. Loci and maximum size of thrust earthquakes and the mechanics of the shallow region of subduction zones, *Tectonics,* **7,** 833–857.

Byrne, D.E., Wang, W. & Davis, D.M., 1993. Mechanical role of backstops in the growth of forearcs, *Tectonics,* **12**(1), 123–144.

Chlieh, M. *et al.*, 2007. Coseismic slip and afterslip of the great Mw 9.15 Sumatra-Andaman earthquake of 2004, *Bull. seism. Soc. Am.,* **97**(1A), S152–S173.

Clift, P. & Vannucchi, P., 2004. Controls on tectonic accretion versus erosion in subduction zones: implications for the origin and recycling of the continental crust, *Rev. Geophys.,* **42,** 2, RG2001.

Curray, J.R., Moore, D.G., Lawver, L.A., Emmel, F.J., Raitt, R.W., Henry, M. & Kieckhefer, R., 1979. Tectonics of the Andaman Sea and Burma, *Am. Assoc. Pet. Geol. Mem.,* **29,** 189–198.

Dahlen, F.A., 1990. Critical taper model of fold-and-thrust belts and accretionary wedges, *Annu. Rev. Earth Planet. Sci.,* **18,** 55–99.

Dessa, J.-X., Klingelhoefer, F., Graindorge, D., Andre, C., Permana, H., Gutscher, M.-A., Chauhan, A., Singh, S.C. & the SUMATRA-OBS Scieic Team, 2009. Megathrust earthquakes can nucleate in the forearc mantle: evidence from the 2004 Sumatra event, *Geology,* **37,** 659–662.

Engdahl, E.R., Villasenor, A., DeShon, H.R. & Thurber, C.H., 2007. Teleseismic relocation and assessment of seismicity (1918–2005) in the region of the 2004 Mw 9.0 Sumatra-Andaman and 2005 Mw 8.6 Nias Island Great earthquakes, *Bull. seism. Soc. Am.,* **97**(1A), S43–S61.

Fisher, D., Mosher, D., Austin Jr., J.A., Gulick, S.P.S., Masterlark, T. & Moran, K., 2007. Active deformation across the Sumatran forearc over the December 2004 M_w9.2 rupture, *Geology,* **35,** 99–102.

Downloaded from https://academic.oup.com/gji/article-abstract/179/3/1772/782446 by CNRS - INSTO user on 06 August 2020

Fuller, C.W., Willet, S.D. & Brandon, T., 2006. Formation of forearc basins and their influence on subduction zone earthquakes, *Geology,* **34,** 65–68.

Graindorge, D. *et al.*, 2008. Impact of lower plate structure on upper plate deformation at the NW Sumatran convergent margin from seafloor morphology, *Earth planet. Sci. Lett.,* **275,** 201–210.

Geist, E.L., Titov, V.V., Arcas, D., Pollitz, F.F. & Bilek, S.L., 2007. Implications of the 26 December Sumatra-Andaman earthquake on tsunami forecast and assessment models for great subduction-zone earthquakes, *Bull. seism. Soc. Am.,* **97,** S249–S270.

Henstock, T.J., McNeill, L.C. & Tappin, D.R., 2006. Sea floor morphology of the Sumatran subduction zone: surface rupture during mega thrust earthquakes?, *Geology,* **34,** 485–488.

Ishii, M., Shearer, P.M., Houston, H. & Vidale, J.E., 2005. Extent, duration and speed of the 2004 Sumatra-Andaman earthquake imaged by the Hi-Net array, *Nature* **435,** 933–936.

Karig, D.E., Lawrence, M.B., Moore, G.F. & Curray, J.R., 1980. Structural framework of the fore-arc basin, NW Sumatra, *J. geol. Soc.,* **137,** 77–91.

Kopp, H. & Kukowski, N., 2003. Backstop geometry and accretionary mechanics of the Sunda margin, *Tectonics,* **22**(6), 1072.

Lallemand, S.E., Schnurle, P. & Malavieille, J., 1994. Coulomb theory applied to accretionary and nonaccretionary wedges: possible causes for tectonic erosion and/or frontal accretion, *J. geophys. Res.,* **99**(B6), 12 033–12 055.

Lin, J.-Y., Le Pichon, X., Rangin, C., Sibuet, J.-C. & Maury, T., 2009. Spatial aftershock distribution of the 26 December 2004 great Sumatra-Andaman earthquake in the northern Sumatra area, *Geochem. Geophys. Geosyst.,* **10**(5), Q05006.

Malod, J.A. & Kemal, B.M., 1996. The Sumatra margin: oblique subduction and lateral displacement of the accretionary prism, *Geol. Soc. Lond. Special Publications,* **106**(1), 19–28.

McCaffrey, R., Zwick, P.C., Bock, Y., Prawirodirdjo, L., Genrich, J.F., Stevens, C.W., Puntodewo, S.S.O. & Subarya, C., 2000. Strain partitioning during oblique plate convergence in northern Sumatra: geodetic and seismologic constraints and numerical modelling, *J. geophys. Res.,* **105,** 28 363–28 376.

McCaughey, M., Barton, P.J. & Singh, S.C., 2000. Joint traveltime inversion of wide-angle seismic data and a deep reflection profile from the central North Sea, *Geophys. J. Int.,* **141,** 100–114.

Plafker, G., Nishenko, S., Cluff, L. & Syahrial, M., 2006. The cataclysmic 2004 tsunami on NW Sumatra - preliminary evidence for a near-field secondary source along the western Aceh Basin, *Seism. Res. Lett.,* **77,** 231.

Platt, J.P., 1989. The mechanics of frontal imbrication: a first-order analysis, *Geol. Rundsch.,* **77,** 577–589.

Prawirodirdjo, L. & Bock, Y., 2004. Instantaneous global plate motion model from 12 years of continuous GPS observations, *J. geophys. Res.,* **109,** B08405.

Robinson, D.P., Henry, C., Das, S. & Woodhouse, J.H., 2001. Simultaneous rupture along two conjugate planes of the Wharton Basin earthquake, *Science,* **292,** 1145–1148.

Scholl, D.W., von Huene, R., Vallier, T.L. & Howell, D.G., 1980. Sedimentary masses and concepts about tectonic processes at underthrust ocean margins, *Geology,* **8,** 564–568.

Schluter, H.U., Gaedicke, C., Roeser, H.A., Schreckenberger, B., Meyer, H., Reichert, C., Djajadihardja, Y. & Prexl, A., 2002. Tectonic features of the southern Sumatra-western Java forearc of Indonesia, *Tectonics,* **21**(5), 1047.

Seeber, L., Mueller, C., Fujiwara, T., Arai, K., Soh, W., Djajadihardja, Y.S. & Cormier, M.-H., 2007. Accretion, mass wasting, and partitioned strain over the 26 Dec 2004 Mw9.2 rupture offshore Aceh, northern Sumatra, *Earth planet. Sci. Lett.,* **263,** 16–31.

Shreve, R.L. & Cloos, M., 1986. Dynamics of sediment subduction, melange formation, and prism accretion, *J. geophys. Res.,* **91**(B10), 10 229–10 245.

Sibuet, J.-C. *et al.*, 2007. 26th December 2004 great Sumatra-Andaman earthquake: co-seismic and post-seismic motions in northern Sumatra, *Earth planet. Sci. Lett.,* **263,** 88–103.

Sieh, K. & Natawidjaja, D., 2000. Neotectonics of the Sumatran fault, Indonesia, *J. geophys. Res.,* **105,** 28 295–28 326.

Singh, S.C. *et al.*, 2005. Sumatra Earthquake Research indicates why rupture propagated northward, *EOS, Trans. Am. geophys. Un.,* **86**(48), 497.

Singh, S.C. *et al.*, 2008. Seismic evidence for broken oceanic crust in the 2004 Sumatra earthquake epicentral region, *Nature Geosci.,* **1**(11), 771–781.

Silver, E.A. & Reed, D.L., 1988. Backthrusting in accretionary wedges, *J. geophys. Res.,* **93,** 3116–3126.

Smith, W.H.F., Scharroo, R., Titov, V.V., Arcas, D. & Arbic, B.K., 2005. Satellite altimeters measure tsunami - early model estimates confirmed, *Oceanography,* **18**(2), 10–12.

Torrini, R.J. & Speed, R.C., 1989. Tectonic wedging in the forearc basin - accretionary prism transition, Lesser Antilles forearc, *J. geophys. Res.,* **94,** 10 549–10 584.

Tréhu, A.M., Asudeh, I., Brocher, T.M., Luetgert, J.H., Mooney, W.D., Nabelek, J.L. & Nakamura, Y., 1994. Crustal architecture of the Cascadia forearc, *Science,* **160**(3), 925–938.

Trinks, I., Singh, S.C., Chapman, C.H., Barton, P.J., Bosch, M. & Cherrett, A., 2005. Adaptive traveltime tomography of densely sampled seismic data, *Geophys. J. Int.,* **266**. no. 5183, 237–2439.

Vita-Finzi, C., 2007. Neotectonics and the 2004 and 2005 earthquake sequences at Sumatra, *Mar. Geol.,* **248,** 47–52.

von Huene, R. & Scholl, D.W., 1991. Observations at convergent margins concerning sediment subduction, subduction erosion, and the growth of continental crust, *Rev. Geophys.,* **29**(3), 279–316.

Wang, W.-H. & Davis, D.M., 1996. Sandbox model simulation of forearc evolution and noncritical wedges, *J. geophys. Res.,* **101**(B5), 329–339.

Wang, K. & Hu, Y., 2006. Accretionary prisms in subduction earthquake cycles: the theory of dynamic Coulomb wedge, *J. geophys. Res.,* **111,** B06410.

Willett, S., Beaumont, C. & Fullsack, P., 1993. Mechanical model for the tectonics of doubly vergent compressional orogens, *Geology,* **21,** 371–374.

Westbrook, G.K., Ladd, J.W., Buhl, P., Bangs, N. & Tiley, G.J., 2006. Cross section of an accretionary wedge: Barbados Ridge complex, *Geology,* **16,** 631.

Downloaded from https://academic.oup.com/gji/article-abstract/179/3/1772/782446 by CNRS - ISTO user on 06 August 2020